

NUMERICAL STUDY OF FLOW IN A 2D BOILER

PETR BAUER*, VLADIMÍR KLEMENT†, PAVEL STRACHOTA†, AND VÍTĚZSLAV ŽABKA†

Abstract. We present a numerical study of flow in a 2D chamber of a simplified industrial boiler. The study features multiple cases of flow with different inlet settings. The mathematical model is based on the incompressible Navier-Stokes equations and solved numerically by means of finite element method. The time discretization is semi-implicit and the resulting linear systems are solved using multigrid solver parallelized via OpenMP. The goal of this study is to provide reference data for a complex model of coal combustion that is being verified.

Key words. Navier-Stokes equations, FEM

AMS subject classifications. 76D05, 76M10

1. Introduction. Our group deals with the development of a complex numerical model of combustion in a pulverized coal fired boiler, introduced in [4],[5]. The model incorporates the equations for 2D compressible turbulent flow, convective and radiative heat transfer, and the reactions of the most important chemical species. Since the publication of [4], the model has been extended in a considerable way in order to simulate various modes of operation of a real device installed at the heat and power plant in Otrokovice, Czech Republic.

To verify the model, several auxiliary tools were created. The one presented in this study is a previously developed FEM code for incompressible flow [2] which was newly adapted to the combustion chamber geometry. The code contains an advanced multigrid solver which, together with the lower complexity of the equation system, allows computations on significantly finer meshes. These computations will help us assess the flow structure and verify the fluid dynamics part of the combustion model.

2. Geometrical settings. Of the many parts of the flue gas duct [1], our model is restricted to the combustion chamber itself. The 2D geometry we use in our computations is the base of an orthogonal prism (Fig. 2.1) that approximates the real shape of the chamber. This 3D model differs from the actual chamber in the lower ash extraction part where the other two walls are inclined. The following quantities are equal in both the real combustion chamber and its model:

- the total volume of the combustion chamber,
- the total area of the surface of the walls,
- the area of a horizontal cut at an arbitrary elevation,
- the cross section of the flue gas outlet.

The chamber contains two types of inlets—burners and *over fire air* (OFA) slots. The burners inject the mixture of pulverized coal and air into the combustion chamber. In the real device, there are six of them in each of the four corners. In the 2D model, we only have six burners on two walls, interpreted in 3D as thin horizontal slits

*Institute of Thermomechanics, Academy of Sciences of the Czech Republic

†Department of Mathematics, Faculty of Nuclear Sciences and Physical Engineering, Czech Technical University in Prague

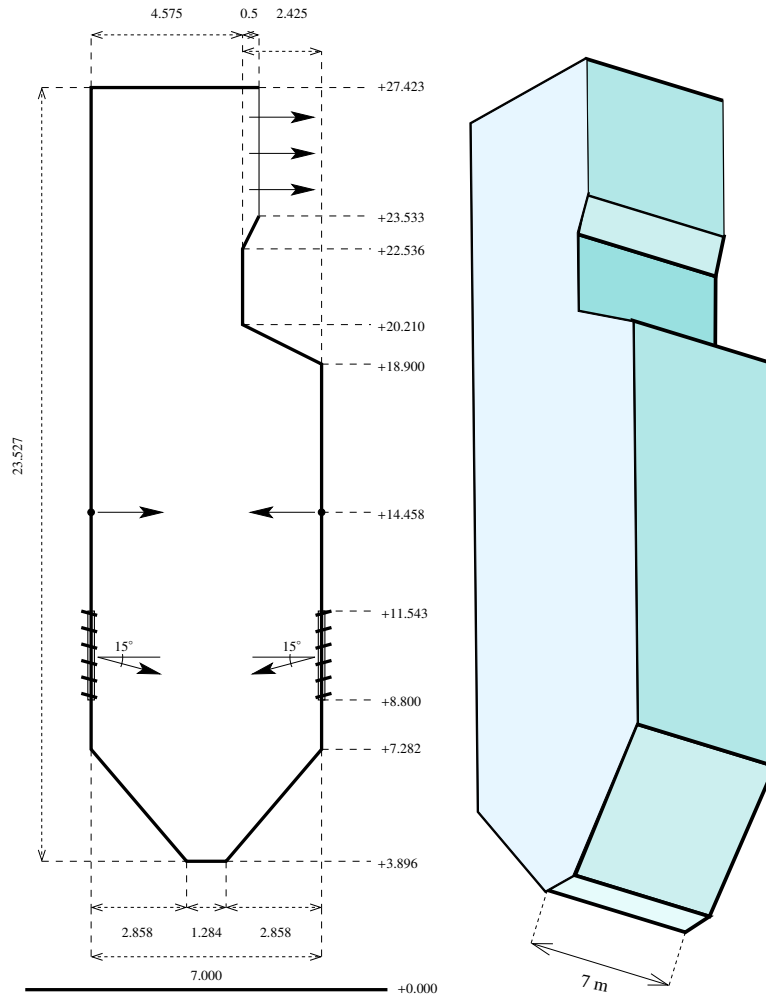


FIG. 2.1. The computational domain (left) and its interpretation in 3D (right). The burners are inclined by 15° from the horizontal plane. Above them, there is one OFA slot on each wall. The flue gas outlet is located in the right wall below the ceiling.

spanning the whole depth of the chamber. Their height is calculated in such a way that the sum of cross sections of all burners is preserved.

The OFA slots are used to inject fresh air several meters above the burner region to reduce the production of NO_x pollutants. The four in-line OFA slots on two opposite walls of the real device are replaced by one inlet on each wall in the 2D model. Their height is calculated analogously as in the case of burners. Finally, there is a flue gas outlet located in the right wall below the ceiling.

3. Mathematical model. Let $\Omega \subset \mathbb{R}^2$ be the computational domain, as shown in Fig. 2.1. On $[0, T] \times \Omega$, we solve the incompressible Navier-Stokes equations for

velocity \mathbf{u} and pressure p , with the kinematic viscosity ν and constant density ρ_0 :

$$\frac{\partial \mathbf{u}(t, \mathbf{x})}{\partial t} + \mathbf{u}(t, \mathbf{x}) \cdot \nabla \mathbf{u}(t, \mathbf{x}) - \nu \Delta \mathbf{u}(t, \mathbf{x}) + \frac{1}{\rho_0} \nabla p(t, \mathbf{x}) = 0, \quad (3.1a)$$

$$\nabla \cdot \mathbf{u}(t, \mathbf{x}) = 0, \quad (3.1b)$$

$$\mathbf{u}(0, \mathbf{x}) = \mathbf{u}_0(\mathbf{x}) \quad \text{in } \Omega, \quad (3.2a)$$

$$\mathbf{u} = 0 \quad \text{on } \Gamma_{\text{wall}}, \quad (3.2b)$$

$$\mathbf{u} = \mathbf{u}_{\text{in}} \quad \text{on } \Gamma_{\text{in}}, \quad (3.2c)$$

$$-p\mathbf{n} + \nu(\nabla \mathbf{u}) \cdot \mathbf{n} = 0 \quad \text{on } \Gamma_{\text{out}}. \quad (3.2d)$$

We prescribe the no-slip boundary condition on the walls of the boiler and the do-nothing boundary condition on the outlet. The burners along with the OFA slots constitute the inlet part with inhomogeneous Dirichlet data. As the initial condition for velocity, we take the stationary Stokes flow with the same boundary conditions.

4. Numerical solution by FEM. We solve the system numerically using the non-conforming P_1/P_0 Crouzeix-Raviart finite elements. The semi-implicit Oseen scheme is used for the time discretization of (3.1a):

$$\frac{\mathbf{u}^n - \mathbf{u}^{n-1}}{\tau} + \mathbf{u}^{n-1} \cdot \nabla \mathbf{u}^n - \nu \Delta \mathbf{u}^n + \nabla p^n = 0, \quad (4.1)$$

where $\tau > 0$ is the time step, $\mathbf{u}^n(\mathbf{x}) \equiv \mathbf{u}(n\tau, \mathbf{x})$ and $p^n(\mathbf{x}) \equiv \frac{1}{\rho_0} p(n\tau, \mathbf{x})$. The convective term is stabilized by upwinding [3]. At each time level n , we solve a linear system of the form

$$\begin{pmatrix} A(\tilde{u}^{n-1}) & B^T \\ B & 0 \end{pmatrix} \begin{pmatrix} \tilde{u}^n \\ \tilde{p}^n \end{pmatrix} = \begin{pmatrix} f(\tilde{u}^{n-1}) \\ g \end{pmatrix}. \quad (4.2)$$

Our method of choice for the solution of (4.2) is the geometric multigrid with Vanka-type smoothers [6]. It works with a nested hierarchy of triangular meshes which are obtained through a uniform refinement of a hand-made coarse mesh; see Fig. 4.1. Vanka-type smoothers are technically block Gauss-Seidel methods where the blocks correspond to all degrees of freedom associated with one element. As a result, the blocks overlap. A typical sequential implementation iterates over the elements, solves the local systems and overwrites the appropriate unknowns with the newly computed values. The result thus depends on the ordering of the elements.

We implemented a parallel version of the solver based on red-black ordering of the elements. Each iteration of the smoother consists of two steps. In the first step, the local systems associated with the red elements are solved in parallel, but only the pressure unknowns are being overwritten. The new values of velocity unknowns are stored separately and an update is performed at the end of the step. Then, the black elements are processed in the same fashion. Our code was parallelized for shared-memory architectures using OpenMP.

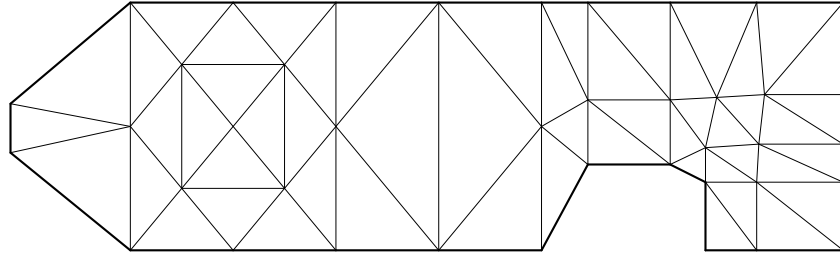


FIG. 4.1. *The coarse mesh. The outlet part of the mesh was extended due to convergence issues.*

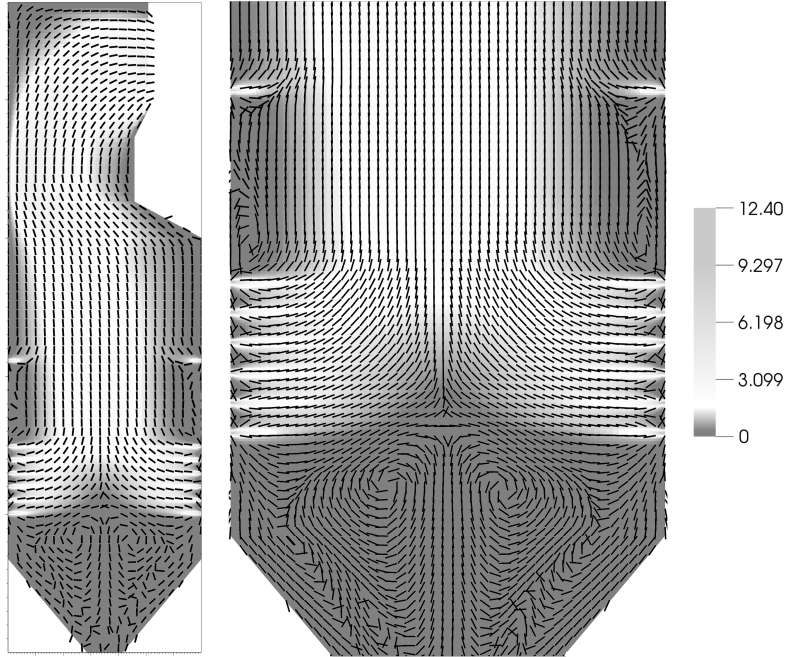


FIG. 5.1. *Combustion model - averaged velocity field with the detail of the burner region.*

5. Numerical studies. Due to its complexity, the combustion model works with coarser grids and employs the $k - \epsilon$ turbulence model to substitute local advective fluxes by means of turbulent diffusivity. In Fig. 5.1, the averaged velocity field is shown for case when no combustion occurs. Only hot air is injected through the burners with the velocity 18 ms^{-1} at the angle 15° downward from horizontal. The OFA velocity is set to 30 ms^{-1} .

The resulting flow looks almost laminar due to the considered parametrization, and its exact behaviour in the vicinity of the burners is below the resolution of the model. To calculate the Reynolds number, we take half of the chamber's width, i.e. 3.5 m , as the characteristic length. With the viscosity $\nu = 3.45 \cdot 10^{-5}$ at 200°C , this yields $Re \approx 1.8 \cdot 10^6$. Such a high value would suggest a strongly turbulent flow with complicated structure.

In order to capture the desired flow structure, we ran multiple series of high-resolution Navier-Stokes simulations using the incompressible model. Because of con-

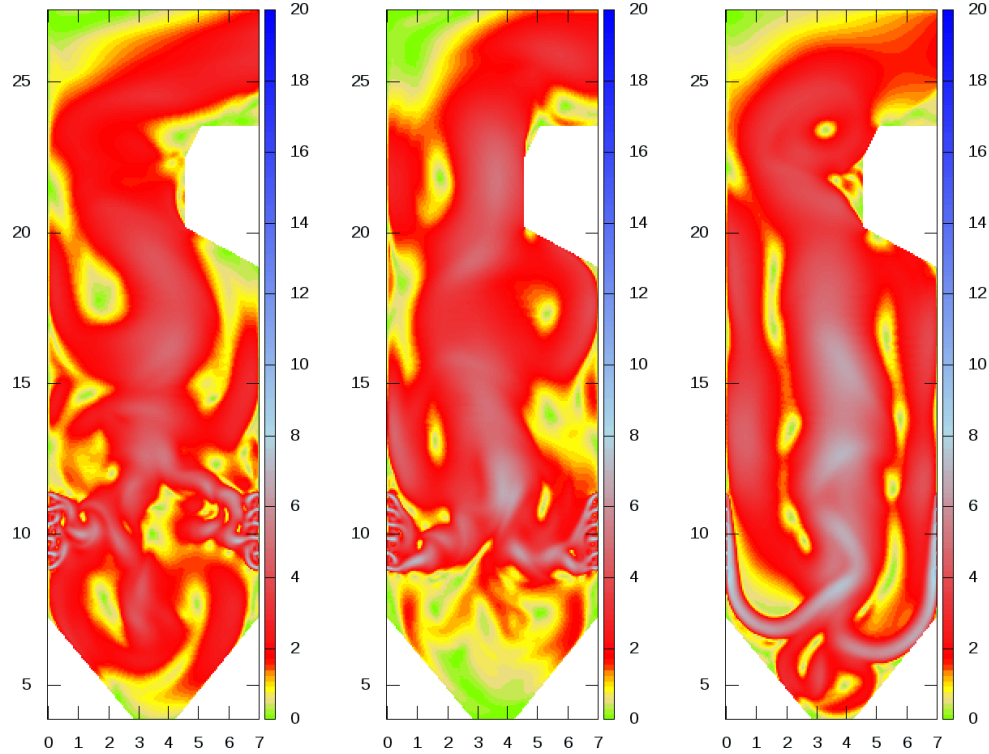


FIG. 5.2. Magnitude of velocity at $t = 12.5$ for inlet angles $0^\circ/15^\circ/45^\circ$.

vergence issues associated with the use of the do-nothing boundary condition, the outlet part of the domain was extended as shown in Fig. 4.1. The total number of degrees of freedom for velocity and pressure combined exceeded three millions. The obtained flow fields were non-stationary throughout the simulations, and the immediate values shown in the figures have illustrative purpose only.

In the first series, three different values of burners angle were tested: 0° , 15° , and 45° , with the inlet velocity set to 20 ms^{-1} ; see Fig. 5.2. In the next series, the angle was fixed at 15° , and the inlet velocities 10 ms^{-1} , 20 ms^{-1} , and 40 ms^{-1} were used on the burners. The timeframes depicted in Fig. 5.3 are taken inversely proportional to the magnitudes of the inlet velocities. The parameters were identical for all burners and stationary for each simulation.

In the last series of simulations, the burners were set to 20 ms^{-1} with 15° angle, and the OFA slots were included. The OFA velocities were ranging from 16 ms^{-1} to 32 ms^{-1} . The results are shown in Fig. 5.4.

6. Conclusion. The results of the study show the complicated character of the flow inside the chamber and its sensitivity to the inlet parameters. This could not be achieved with the combustion model alone, as its results visually correspond to flows with $Re \approx 100$, before transition to turbulence. Direct solution of Navier-Stokes equations for high Reynolds numbers was therefore needed.

Our FEM code for incompressible Navier-Stokes flow proved sufficient for the task, though the OpenMP parallelization helped only partially. On a 24-core system, the speedup of approximately five was achieved compared to the original sequential implementation. The code is being further developed and will mainly be used

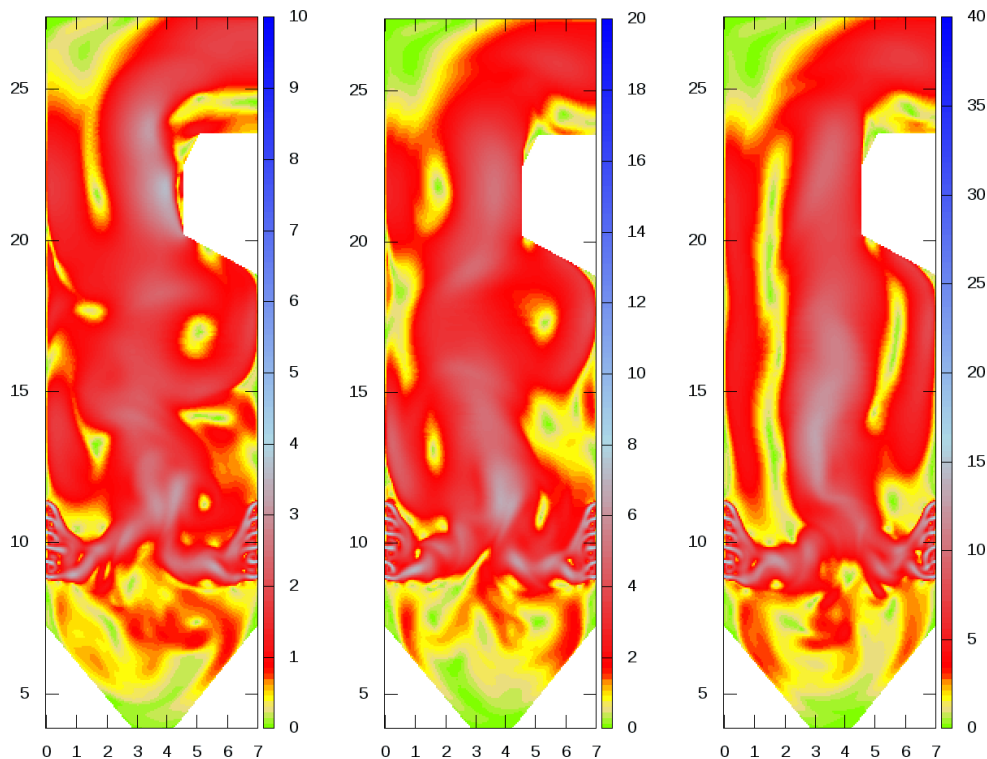


FIG. 5.3. Magnitude of velocity at $t = 25/12.5/6.25$ for inlet velocities 10/20/40.

for its original application of simulating air flow and dispersion of pollutants in the atmospheric boundary layer.

Acknowledgments. The support of the project No. TA01020871 of the Technological Agency of the Czech Republic, the grant No. SGS11/161/OHK4/3T/14 of the Student Grant Agency of the Czech Technical University in Prague, and the project COST LD12007 of the Ministry of Education, Youth and Sports of the Czech Republic is acknowledged.

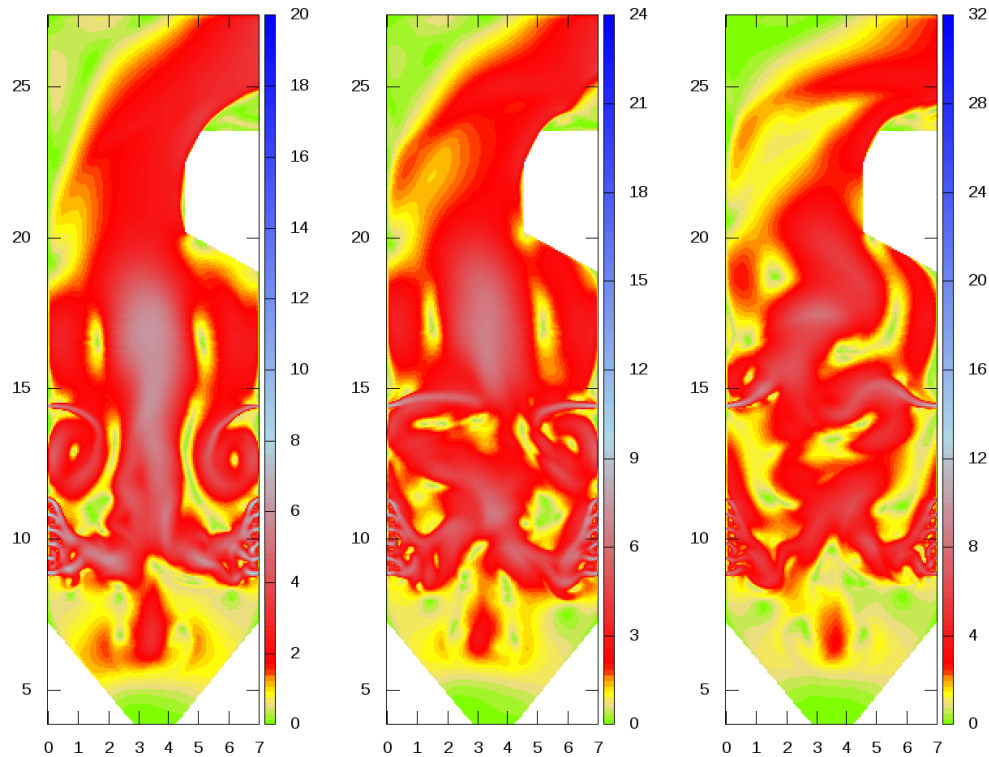


FIG. 5.4. Magnitude of velocity at $t = 6.25$ for OFA velocities 16/24/32.

REFERENCES

- [1] P. BASU, C. KEFA AND L. JESTIN, *Boilers and Burners: Design and Theory*, Springer, 1999.
- [2] P. BAUER, *Mathematical modelling of flow over periodic structures*, COE Lecture Note, 36 (2012), pp. 3–10.
- [3] F. SCHIEWECK AND L. TOBISKA, *An optimal order error estimate for upwind discretization of the Navier-Stokes equation*, Numerical methods in partial differential equations, 12(4) (1996), pp. 407–421.
- [4] R. STRAKA AND M. BENEŠ, *Numerical simulation of NO production in air-staged pulverized coal fired furnace*, The Open Thermodynamics Journal, 4 (2010), pp. 27–35.
- [5] R. STRAKA, J. MAKOVÍČKA AND M. BENEŠ, *Numerical simulation of NO production in pulverized coal fired furnace*, Environment Protection Engineering, 37(2) (2011), pp. 13–22.
- [6] V. JOHN, *On the Parallel Performance of Coupled Multigrid Methods for the Solution of the Incompressible Navier-Stokes Equations*, Large Scale Scientific Computations of Engineering and Environmental Problems, 62 (1998), pp. 269–280.